

Flow past a Square Cylinder at Small Incidence Angles: Characteristics of Leading Three-Dimensional Instabilities

Gregory J Sheard

Department of Mechanical and Aerospace Engineering, Monash University, VIC 3800, Australia

Greg.Sheard@monash.edu

Abstract – A detailed linear stability analysis is conducted on the flow past a square cylinder inclined at an angle to an oncoming flow. At shallow incidence angles two distinct three-dimensional instabilities present as the first-occurring modes in the wakes with increasing Reynolds number. At incidence angles below 10.5 degrees, the flow becomes three-dimensional via the classical Mode A instability seen behind circular cylinders. However, at higher incidence angles the wake experiences a period-doubling bifurcation as a subharmonic instability develops in place of the Mode A wake.

Index Terms – Square cylinder, three-dimensional, wake instabilities.

I. INTRODUCTION

The flow past a square cylinder serves as a model for myriad applications in engineering, including offshore structures, buildings, bridges and pylons. These flows are characterized by the Reynolds number, which relates inertial to viscous effects in a flow. At low Reynolds numbers the flow is steady and laminar, and at higher Reynolds numbers the flow transitions first to time-dependent flow and then to three-dimensional flow, before eventually becoming turbulent. Three-dimensional transition in the flow past cylinders leads to abrupt changes in vortex shedding frequency and both lift and drag characteristics. It is therefore of interest as these transitions can have serious implications for the predictions of loading and fatigue of structures.

A useful method for analysis of three-dimensional transition in wake flows is linear stability analysis, which yields growth rates (σ) for linear three-dimensional instability modes with given spanwise wavelength λ growing on a two-dimensional base flow. A Floquet linear stability analysis was conducted by [1] on the wake of a circular cylinder. Their analysis accurately predicted the critical Reynolds number, spanwise wavelength, and spatio-temporal symmetry of the first-occurring three-dimensional instability, and their predictions matched very well to laboratory observations [2, 3]. Mode A emerges at a Reynolds number (based on freestream velocity and cylinder diameter) of $Re \approx 180$ -190, and it is characterized by a spanwise wavelength approximately 4 times the cylinder diameter. The wake subsequently transitions to a second three-dimensional mode (Mode B), over $Re \approx 230$ -260, which is characterized by a shorter spanwise wavelength of approximately 1 cylinder diameter. This second mode was also predicted by [1].

These modes have subsequently been found to be common to other extruded geometries, such as slender rings facing an oncoming flow [4, 5], staggered tandem circular cylinders [6],

and cylinders with square cross-section [7, 8]. For these geometries, Mode A is usually observed at a lower Reynolds number than Mode B. In addition, a number of studies have also detected a third instability mode in these systems. For circular cylinders [9] and square cylinders at zero incidence [8], a quasi-periodic mode is predicted, whereas behind rings [10, 11] and inclined square cylinders [12, 13], a subharmonic mode is predicted. These modes are distinguished by their temporal properties arising from the respective eigenvalues of the evolution operator of the linearized Navier—Stokes equations used to determine the stability of the flow. A subharmonic eigenvalue lies on the negative real axis, whereas a quasi-periodic mode occurs as a complex-conjugate pair. A subharmonic mode invokes a period-doubling of the flow once the instability develops, whereas a quasi-periodic mode has the physical effect of introducing a new frequency into the flow. Analysis by [14] has shown that quasi-periodic modes are permitted in flows exhibiting a half-period reflective symmetry about the wake centreline (e.g. a square cylinder at zero incidence), whereas those systems do not allow a subharmonic mode. In contrast, subharmonic modes are permitted in systems which break this symmetry (e.g. an inclined square cylinder).

The system under investigation is shown in Fig. 1. It comprises a cylinder with a square cross-section inclined at an angle α to the oncoming flow, placed perpendicular to a uniform flow with speed U . The square cross-section has side length d , and the characteristic length is taken to be the projected height of the cylinder facing the oncoming flow, h . This gives a Reynolds number

$$Re = \frac{Uh}{\nu},$$

where ν is the kinematic viscosity of the fluid. The control parameters for the system are Re and α .

Laboratory investigations have previously investigated square cylinders at both a zero incidence [15] and at inclination [16]. These studies employed dye visualization and hot-wire measurements to elucidate transitions in the flow, and proposed the first map of two- and three-dimensional regimes in the Reynolds number-incidence angle parameter space for inclined square cylinders. A linear stability analysis [12], supported by direct numerical simulation, determined that the first-occurring three-dimensional transition behind inclined square cylinders was Mode A at incidence angles near 0° and 45° , and a subharmonic mode (Mode C) at intermediate angles. The subharmonic mode was most unstable at approximately $\alpha \approx 25^\circ$, and the transition Reynolds number

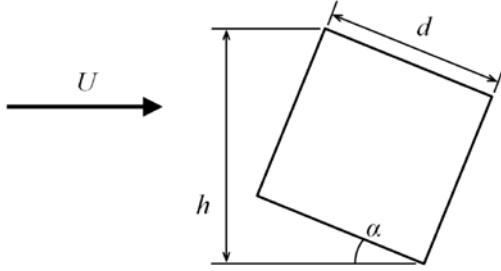


Fig. 1 A schematic representation of the inclined square-cylinder system, showing inclination angle α , characteristic length scale h , and free-stream velocity U .

increased substantially towards both 0° and 45° . At a zero incidence angle, [8, 12] identified a quasi-periodic mode, which was predicted to become unstable well above the critical Reynolds numbers for Modes A and B, but no evidence was found for the quasi-periodic mode at non-zero incidence angles. However, that analysis was only conducted at 7.5° increments in incidence angle, which raised a question as to whether the subharmonic mode immediately replaces the quasi-periodic mode the instant that the wake symmetry is broken at non-zero incidence angles, or whether the quasi-periodic mode persists at small non-zero angles.

Ref. [17] sought to address this question by investigating the effect of breaking reflective wake centreline symmetry at small increments. It was found that the quasi-periodic mode persisted while the symmetry-breaking was small but finite, and as it was further increased the complex-conjugate pair of eigenvalues smoothly migrated towards the negative real axis where it split into a pair of subharmonic eigenvalues. This study demonstrated that with increasing incidence angle, the quasi-periodic mode *changes into* the subharmonic mode, rather than being *replaced* by it through the emergence of a distinct eigenvalue.

A more recent numerical study [13] calculated the stability of an inclined square cylinder flow at a number of additional incidence angles, refining the Reynolds number-incidence angle regime map. Two notable features arose from their results: firstly, in keeping with the results of [17], the quasi-periodic mode branch was found to extend to non-zero incidence angles (they detected the quasi-periodic mode up to approximately 2° , but included no data on the quasi-periodic/subharmonic branch up to $\alpha = 10.2^\circ$), and secondly, while interpolation suggested in [12] that the crossover from Mode A to the subharmonic mode occurred at approximately 12° , [13] detected the subharmonic mode and not Mode A at a lower angle of 10.2° . Thus [12] over-estimated the threshold incidence angle for the crossover from Mode A to the subharmonic mode, and considering the data in [13], the crossover could potentially occur anywhere down to 7.5° . Furthermore, why is Mode A not detected at all at $\alpha = 10.2^\circ$? The present study addresses these questions through a more detailed stability analysis of the inclined square cylinder wake.

II. NUMERICAL TREATMENT

A two-dimensional code [18, 19] employing a nodal spectral element method for spatial discretization and a third-

order time integration scheme based on backwards differentiation is used to solve the time-dependent incompressible Navier—Stokes equations. Linear stability analysis is performed by evolving a three-dimensional perturbation on the two-dimensional base flow using the linearized Navier—Stokes equations [1]. Stability eigenvalues are determined using the ARPACK package [20], where the complex eigenvalues are Floquet multipliers (μ), and eigenvectors give the instability mode shape (for details see [12, 17]). Floquet multipliers represent amplification factors, and relate to the exponential growth rates (σ) of modes through $\sigma = \log|\mu|/T$, where T is the temporal period of the base flow. A Floquet multiplier with $|\mu| > 1$ corresponds to a positive growth rate ($\sigma > 0$) and an unstable mode.

The meshes employed here were adapted from those employed for the square-cylinder calculations in [17]. The domain size and element distribution were maintained for all incidence angles. The meshes have 644 elements with a polynomial degree 9. The distances from the cylinder to the upstream, transverse, and downstream boundaries were $20h$, $20h$, and $35h$, respectively. On all boundaries except the downstream boundary a high-order Neumann pressure gradient boundary condition was imposed to preserve the third-order time accuracy of the computations [21], and on the downstream boundary a constant reference pressure was imposed. A uniform horizontal velocity was imposed at the upstream boundary, and stress-free conditions were imposed on the transverse boundaries. A no-slip condition was imposed on velocity at the surface of the cylinder, and a zero normal gradient of velocity was weakly imposed naturally on the downstream boundary by the Galerkin treatment of the diffusion sub-step of the time integration scheme.

The aim of this study is to develop a detailed map of transition regimes at small incidence angles. Hence incidence angles over $0^\circ \leq \alpha \leq 12^\circ$ are computed at approximately 1° increments. Analysis was targeted at narrow ranges of Reynolds numbers and spanwise wavelengths surrounding the dominant modes, minimising the intervals between data points and enhancing the precision of the predictions. Polynomial curve fitting was used to determine the wavenumber m (which relates to the spanwise wavelength through $\lambda/h = 2\pi/m$) corresponding to the peak growth rate for an instability mode at a given Reynolds number, and interpolation was performed to find the critical Reynolds number and wavenumber at which the mode first becomes neutrally stable (i.e., zero growth rate). Typically, 15 to 20 Floquet multipliers were computed to obtain each critical Reynolds number in the results to follow.

III. RESULTS

A. The Mode A Branch

Fig. 2 shows the key Reynolds number curves for the Mode A instability branch at small angles. At $\alpha = 0^\circ$, the present stability calculations for the onset of the Mode A instability are in agreement with [12], predicting $Re_{\text{crit}} = 164$ at a wavenumber $m = 1.24$. With an increase in α , the critical Reynolds number for the onset of the Mode A instability also

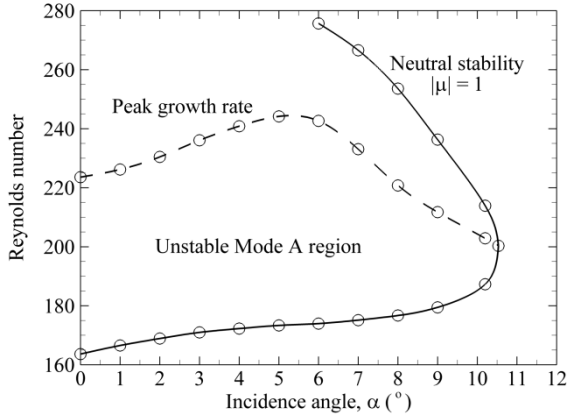


Fig. 2 Critical Reynolds numbers for the Mode A instability plotted against incidence angle. The unstable region of the parameter space is shaded, and a dashed line marks the point at which the maximum growth rate was found in the Mode A waveband for each incidence angle.

increases. Unusually, for a given α , the growth rate reached a maximum value, before subsequently decreasing again at higher Reynolds numbers. The Reynolds number for peak for Mode A growth rate is predicted to be $Re = 224$ at $\alpha = 0^\circ$; it increases to $Re = 244$ at $\alpha \approx 5^\circ$, and at higher incidence angles the peak occurs at lower Reynolds numbers. With increasing incidence angle, the Mode A instability was unstable over a decreasing range of Reynolds numbers. These computations predict that by $\alpha = 10.5^\circ$, the Mode A waveband is not unstable for any Reynolds numbers considered in this study. At $\alpha = 10.5^\circ$, the critical Reynolds number at which Mode A grazes the neutral stability threshold is $Re = 200$. This shows that the flow becomes less sensitive to the Mode A instability as the incidence angle is increased from 0° .

The achievement of positive growth rates for the Mode A instability in these computations at $\alpha = 10.2^\circ$ (and indeed up to $\alpha = 10.5^\circ$) is in contrast to the calculations in [13], where Mode A was not detected at $\alpha = 10.2^\circ$. Given the close (but not exact) agreement between their critical Reynolds number curves and those of [12], the differences between the two sets of computations may be attributed to the different domain sizes and numerical techniques employed in the two studies. It is highly likely that the suppression of Mode A observed in the present calculations most likely occurred at an incidence angle just below $\alpha = 10.2^\circ$ in their model, which explains their detection of only the subharmonic (Mode C) instability at that incidence angle.

B. Subharmonic and Quasi-Periodic Modes

The critical Reynolds number curve for the quasi-periodic/subharmonic mode branch is shown in Fig. 3. Ref [17] showed that the transition from quasi-periodic to subharmonic eigenvalues occurred at an incidence angle of $\alpha = 5.9^\circ$ for a cylinder with a square cross-section. That study conducted the stability analysis at a constant Reynolds number (based on the cylinder side length) of $Re_d = 225$. At $\alpha = 5.9^\circ$, this corresponds to a Reynolds number here of $Re = 247$. At that Reynolds number the Floquet multiplier resided inside the unit circle ($|\mu| < 1$), which corresponds to a decaying mode

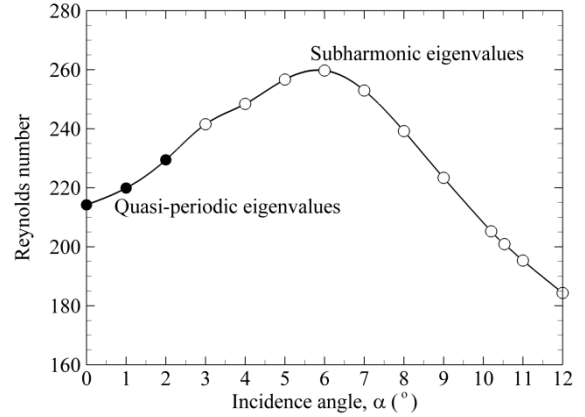


Fig. 3 Critical Reynolds numbers for the quasi-periodic and subharmonic modes plotted against incidence angle. Black and white symbols denote modes with quasi-periodic and subharmonic eigenvalues, respectively.

and a stable flow. In this study eigenvalues are determined at precisely the transition Reynolds number and peak wavenumber for all incidence angles. At the critical Reynolds number, the shift from quasi-periodic to subharmonic mode characteristics occurs somewhere between $\alpha = 2^\circ$ and 3° , in good agreement with [13], which detected a quasi-periodic mode at $\alpha \approx 2^\circ$.

At $\alpha = 0^\circ$, the mode has a critical Reynolds number of $Re_c = 214$, consistent with [12]. The critical Reynolds number increases with incidence angle to a maximum of $Re_c \approx 260$ at $\alpha \approx 6^\circ$, before subsequently decreasing with further increases in α . The trend of the critical Reynolds number rising over $0^\circ \leq \alpha < 6^\circ$ and falling beyond $\alpha \approx 6^\circ$ closely mirrors the trend in the maximum growth rate of the Mode A instability.

Highlighting the consistency across the quasi-periodic and subharmonic states, Fig. 4 shows the perturbation fields at several incidence angles along the neutral stability curve. The topologies of the perturbation field mode structures are qualitatively consistent across these incidence angles, supporting the view that the quasi-periodic and subharmonic regimes are part of the one mode branch. No sudden change in structure is detected through the switch between these regimes.

IV. SUMMARY AND CONCLUSIONS

This study provides a clearer description of the stability of the wake behind an inclined square cylinder than is available from earlier attempts to map these regimes [12, 13]. The updated regime map is plotted in Fig. 5. This study demonstrates that with increasing incidence angle from $\alpha = 0^\circ$, the flow is first unstable to the Mode A instability. This mode is progressively suppressed, so that by $\alpha = 10.5^\circ$ the flow is no longer unstable to Mode A. Thereafter, the first-occurring instability is the subharmonic Mode C instability. As the incidence angle approaches 45° , which corresponds to a recovery of reflective symmetry about the wake centreline, [12] showed that Mode C is replaced again by Mode A as the first-occurring instability mode.

ACKNOWLEDGMENT

This work was supported by a Monash University Faculty of Engineering Small Grant. Simulations were performed using the resources of the NCI National Facility, which is supported by the Australian Commonwealth Government.

REFERENCES

- [1] D. Barkley, and R.D. Henderson, "Three-dimensional Floquet stability analysis of the wake of a circular cylinder," *Journal of Fluid Mechanics*, vol. 322, pp. 215–241, 1996.
- [2] C.H.K. Williamson, "The existence of two stages in the transition to three-dimensionality of a cylinder wake," *Physics of Fluids*, vol. 31, pp. 3165–3168, 1988.
- [3] C.H.K. Williamson, "Mode A secondary instability in wake transition," *Physics of Fluids*, vol. 8, pp. 1680–1682, 1996.
- [4] G.J. Sheard, M.C. Thompson, and K. Hourigan, "From spheres to circular cylinders: The stability and flow structures of bluff ring wakes," *Journal of Fluid Mechanics*, vol. 492, pp. 147–180, 2003.
- [5] G.J. Sheard, M.C. Thompson, and K. Hourigan, "From spheres to circular cylinders: Non-axisymmetric transitions in the flow past rings," *Journal of Fluid Mechanics*, vol. 506, pp. 45–78, 2004.
- [6] B.S. Carmo, S.J. Sherwin, P.W. Bearman, and R.H.J. Willden, "Wake transition in the flow around two circular cylinders in staggered arrangements," *Journal of Fluid Mechanics*, vol. 597, pp. 1–29, 2008.
- [7] J. Robichaux, S. Balachandar, and S.P. Vanka, "Three-dimensional Floquet instability of the wake of a square cylinder," *Physics of Fluids*, vol. 11, pp. 560–578, 1999.
- [8] H.M. Blackburn, and J.M. Lopez, "On three-dimensional quasi-periodic Floquet instabilities of two-dimensional bluff body wakes," *Physics of Fluids* vol. 15, pp. L57–L60, 2003.
- [9] H.M. Blackburn, F. Marques, and J.M. Lopez, "Symmetry breaking of two-dimensional time-periodic wakes," *Journal of Fluid Mechanics*, vol. 522, pp. 395–411, 2005.
- [10] G.J. Sheard, M.C. Thompson, K. Hourigan, and T. Leweke, "The evolution of a subharmonic mode in a vortex street," *Journal of Fluid Mechanics*, vol. 534, pp. 23–38, 2005.
- [11] G.J. Sheard, M.C. Thompson, and K. Hourigan, "The subharmonic mechanism of the Mode C instability," *Physics of Fluids*, vol. 17, article no. 111702, 2005.
- [12] G.J. Sheard, M.J. Fitzgerald, and K. Ryan, "Cylinders with square cross section: Wake instabilities with incidence angle variation," *Journal of Fluid Mechanics*, vol. 630, pp. 43–69, 2009.
- [13] D.H. Yoon, K.S. Yang, and C.B. Choi, "Flow past a square cylinder with an angle of incidence," *Physics of Fluids*, vol. 22, article no. 043603, 2010.
- [14] F. Marques, J.M. Lopez, and H.M. Blackburn, "Bifurcations in systems with Z_2 spatio-temporal and $O(2)$ spatial symmetry," *Physica D*, vol. 189, pp. 247–276, 2004.
- [15] S.C. Luo, X.H. Tong, and B.C. Khoo, "Transition phenomena in the wake of a square cylinder," *Journal of Fluids and Structures*, vol. 23, pp. 227–248, 2007.
- [16] X.H. Tong, S.C. Luo, and B.C. Khoo, "Transition phenomena in the wake of an inclined square cylinder," *Journal of Fluids and Structures*, vol. 24, pp. 994–1005, 2008.
- [17] H.M. Blackburn, and G.J. Sheard, "On quasi-periodic and subharmonic Floquet wake instabilities," *Physics of Fluids*, vol. 22, article no. 031701, 2010.
- [18] G.J. Sheard, T. Leweke, M.C. Thompson, and K. Hourigan, "Flow around an impulsively arrested circular cylinder," *Physics of Fluids*, vol. 19, article no. 083601, 2007.
- [19] A. Neild, T.W. Ng, G.J. Sheard, M. Powers, and S. Oberti, "Swirl mixing at microfluidic junctions due to low frequency side channel fluidic perturbations," *Sensors and Actuators B: Chemical*, vol. 150, no. 2, pp. 811–818, 2010.
- [20] R.B. Lehoucq, D.C. Sorenson, and C. Yang, *ARPACK Users' Guide*. SIAM: Philadelphia, PA., 1998.
- [21] G.E. Karniadakis, M. Israeli, and S.A. Orszag, "High-order splitting methods for the incompressible Navier-Stokes equations," *Journal of Computational Physics*, vol. 97, pp. 414–443, 1991.

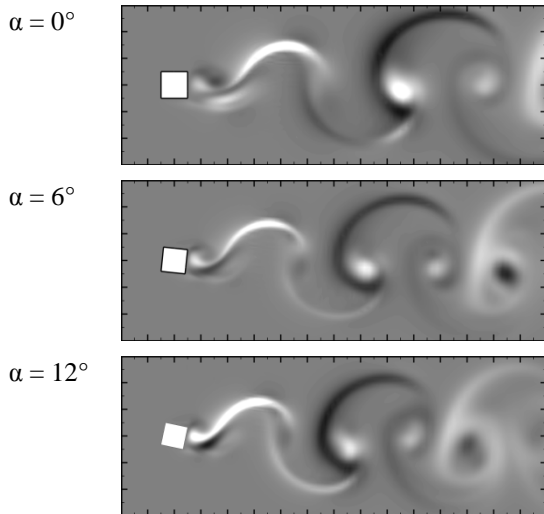


Fig. 4 Contour plots of the horizontal component of velocity in the perturbation field of the dominant mode in the quasi-periodic/subharmonic waveband at the neutral stability threshold (the curve in Fig. 3) at several incidence angles. Light and dark shading correspond to positive and negative velocities, respectively.

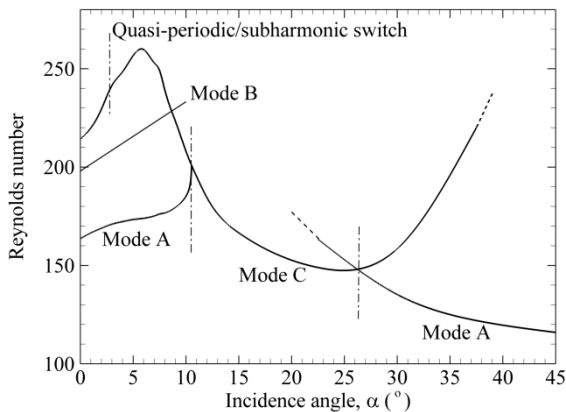


Fig. 5 The updated regime map for linear instability modes in the wakes behind inclined square cylinders, with critical Reynolds number curves plotted against incidence angle. The various modes are labelled, and dash-dotted lines are used to mark important incidence angles in the parameter space. The terms "QP" and "C" refer to the quasi-periodic and subharmonic (Mode C) parts of that transition curve.

This study also shows the critical Reynolds number curve for the quasi-periodic mode branch to be unbroken. While this mode is not the first-occurring instability for $\alpha < 10.5^\circ$, and therefore may not be detectable at these incidence angles in a physical setting, this finding is important from the perspective of understanding the relationship between quasi-periodic and subharmonic instability modes in generic time-periodic flows exhibiting the same spatio-temporal symmetry properties as these flows.

This study has also shown that at the critical Reynolds number, the switch from quasi-periodic to subharmonic properties occurs between $\alpha \approx 2^\circ$ and 3° . The combination between these results and those in [17] could potentially be used to seek a universal criterion for the critical amount of asymmetry required to invoke the subharmonic switchover.